HyGage: Solving the Hysteresis Puzzle with a New Streamflow Monitoring Method

Marian Muste[1], Kyeongdong Kim[1], Alexandre Hauet[2], Christophe Rousseau[3], Emma House[4], Ehab Meselhe[4], Ibrahim Demir[4]

[1]IIHR-Hydroscience & Engineering, The University of Iowa, Iowa City, IA, USA

[2]Institut des Géosciences de l'Environnement (IGE) - Équipe Hydrimz, Université Grenoble Alpes, Grenoble, France

[3]University of Grenoble Alpes, IRD, CNRS, INRAE, Grenoble INP, IGE, Grenoble, France

[4]Department of River-Coastal Science and Engineering, School of Science and Engineering, Tulane University, New Orleans, LA, USA

Abstract

The questionable reliability of discharges obtained using the traditional stage–discharge method under gradually varied flow conditions continues to motivate the search for improved monitoring approaches that support water resources management, streamflow forecasting, and multipurpose scientific investigations related to the water cycle. This paper introduces HyGage, a new physically based monitoring method grounded in the governing equations of spatiotemporal, gradually varied, shallow open channel flow. The methodology integrates measurement elements commonly employed in the index velocity and slope area methods within a unified analytical framework, enabling real time discharge estimation in both steady and gradually varied flows without relying on the semi empirical techniques of the past. The performance of HyGage is evaluated by comparing its discharge estimates with those obtained from established methods. Unlike conventional approaches, HyGage is not built around any specific instrument; instead, it can flexibly incorporate combinations of immersed, close range, and remote sensing measurements through seamless integration.

Keywords: gradually-varied flows, streamflow monitoring, stage-discharge rating, index-velocity method, slope-area method, hybrid gaging method (HyGage)

Introduction

The automated monitoring of flow rates in rivers is the result of more than a century-long development with the goal of supporting observations and investigations on the water cycle for a myriad of practical and scientific uses. The oldest streamflow monitoring method is the stage-discharge rating curve (labeled herein HQRC) which continues to be widely used worldwide because it is easier to deploy and operate compared to other approaches. The major HQRC limitation is the time-wise, quasi-steady flow assumption applied uniformly for observing flows using a single hydraulic variable, the flow depth. The flow depth is typically derived from the measurement of water surface level (a.k.a. stage) from a local gage datum. The HQRC performance is totally acceptable for quasi steady and uniform flows, conditions that are attained between precipitation events when the river is at its base flow. The base flow persistence in perennial rivers is directly related to the climatic and hydrological settings of the monitoring site. Most of the monitoring sites located in temperate and continental climates are exposed to slow evolving, sporadic spatial changes of river morphology and shorter and more frequent temporal changes in the flow regimes triggered by precipitation events passing through the station.

The large-scale morphological changes occur at stream-reach scales and are produced by processes that mainly affect the longitudinal river profile (e.g., migration, avulsion, vegetation growth). There are also local (cross-sectional) morphological changes that occur in the vicinity of a river gaging site (e.g., erosion, deposition, bank failure). Natural morphological changes are often compounded with those produced by man-made hydraulic structures installed in the stream (e.g., locks, dams, bridge abutments). Morphological changes downstream the station leads to steady and non-uniform flows in the stream reach, resulting in flow storage. The stream-reach and cross-sectional morphological changes can act simultaneously making their detection complex and costly due to the need for recursive gaging site inspections (Darienzo et al., 2021). Morphological changes at any scale can modify or even shift the hydraulic regimes at the station (by changing the flow control from channel to local) and/or create areas of backwater that affect the validity of the originally constructed ratings (Herschy, 2009). Temporal changes in the flow regimes at a station are produced by runoff entering the stream or changes in the operation regimes at hydraulic structures installed upstream the station. Temporal changes produce unsteady and non-uniform flows during fluvial wave passages.

In the present context, we use the term **Unsteady Gradually Varied Flow (UGVF)** to describe the spatiotemporal flow changes occurring at a gaging station and to distinguish them from the conventional **Gradually Varied Flow (GVF)** associated with non-uniform steady flows. Both UGVFs and GVFs alter the water-surface profile near the gaging station. However, UGVFs are not explicitly accounted for in current monitoring protocols based on stage, index-velocity, or free-slope measurements, which assume quasi-steady flow conditions over time. Consequently, these methods do not differentiate between the flow mechanisms acting on the rising and falling limbs of hydrographs during UGVFs and those occurring under steady-flow conditions (Muste et al., 2025b).

Propagation of UGVFs through gaging stations involves both flow storage and flow unsteadiness near the measurement site (Rantz et al., 1982; Dykstra & Dzwonkowski, 2020). These variations produce **hysteretic behavior**, a nonlinear phenomenon in which the system state depends not only on current inputs but also on the sequence of prior conditions that led to that state (Prowse, 1984). Hysteresis is also observed in magnetism and in electrical and mechanical systems, where it can be described mathematically for deterministic signals (Ikhouane, 2013) or analytically when the governing physical laws are known. In open-channel flows, hysteresis arising from spatiotemporal variability is both widespread and persistent; in temperate inland rivers, unsteady-flow conditions may prevail for more than 50% of annual flow conditions (Muste et al., 2025a).

The simple **HQRC** method is particularly susceptible to UGVF-induced hysteresis because it assumes a unique stage-discharge relationship. In reality, the intrinsic dynamics of UGVFs produce non-unique, hysteretic relationships among hydraulic variables, especially during high-magnitude, flashy events in lowland rivers (Dottori et al., 2009; Muste et al., 2020; Muste et al., 2025a). Persisting with the assumption of unique hydraulic relationships during unsteady flows disregards well-established open-channel flow physics and introduces **epistemic uncertainty** into streamflow estimation (Schmidt, 2002; Beven, 2016). These uncertainties compound other sources of measurement error (Di Baldassarre & Montanari, 2009; Westerberg & Karlsen, 2024), reducing the reliability of streamflow records, particularly during extreme events (Dottori et al., 2018; Kreibich et al., 2022), when accurate data are most critical for flood assessment and water-resource management (McMillan et al., 2017).

Streamflow-monitoring agencies have long recognized the limitations of real-time HQRC estimates and have sought to address UGVF and GVF effects through correction methods based on auxiliary ratings, analytical formulations, and numerical simulations (Muste et al., 2025b). Despite their demonstrated value, these correction methods are applied only sporadically and inconsistently in real-time operations because they require additional measurements, increased costs, and, in many cases, lack a compelling cost-benefit justification. Consequently, real-time streamflow records at most U.S. HQRC gaging stations are designated as "provisional" until they can be reviewed for rating shifts caused by channel changes and corrected for unsteadiness and backwater effects (USGS, 2010). Following periodic quality-control reviews, typically conducted at approximately six-month intervals, the data are reclassified as "final" and assumed to reflect the cumulative effects of the processes not explicitly accounted for in real-time reporting.

The limited availability of systematic experimental evidence on the severity of hysteretic effects in natural streams, coupled with the substantial cost and effort required to document these effects comprehensively, has resulted in a status quo in which HQRC operated in UGVFs and GVFs often remain unaddressed. This inaction can markedly degrade data accuracy, especially when real-time data is needed at sub-daily sampling intervals (Beven, 2006; Holmes, 2016). Recognizing these limitations, monitoring agencies have sought to improve the reliability of discharge estimation by testing and implementing alternative approaches, such as the Index-Velocity method (IVRC) and the Continuous Slope-Area method (CSA). The adoption of these methods has been facilitated by advances in measurement technologies that occurred after 1980s - particularly the emergence of acoustic sensing instruments (Laenen, 1985; ISO 1070:1992 - superseded by ISO 1070:2018). Nevertheless, comprehensive evaluations of HQRC-based corrections as well as of the IVRC, and CSA methods remain ongoing, as their comparative performance continues to be critically examined (e.g., Muste et al., 2025b).

Motivated by persistent challenges in streamflow monitoring, particularly under flash-flood conditions, and by the growing availability of advanced sensing technologies, including acoustic, radar, and image-velocimetry systems (Tsubaki et al., 2025), we developed a new hybrid monitoring approach, **HyGage** (Muste et al., 2023), which is the subject of a patent application (USPTO, 2026). This paper first reviews the IVRC and CSA method components that form the foundation of the HyGage framework. It then presents the conceptual basis of the framework and, for the first time, demonstrates its performance in monitoring UGVFs using a customized instrumentation configuration deployed at the Clear Creek gaging station in Oxford, Iowa (USA). Finally, we illustrate how HyGage reduces key conceptual uncertainties inherent in conventional streamflow-monitoring methods and highlight the new capabilities and opportunities enabled by its adoption.

METHODS

General Considerations

The newly introduced HyGage concept draws inspiration from and integrates in an innovative manner, measurement components of the IVRC and CSA methods. HyGage development was motivated by a growing body of observational evidence from IVRC and CSA stations, as these data sets showed that augmenting traditional stage measurements—which describe the geometric state of channel flow—with additional hydraulic variables such as index velocity or free-surface slope provides a more realistic representation of flow dynamics compared with the steady HQRC method. This enriched flow descriptions have been shown to improve the accuracy of monitored discharge and enhance the predictive capability for UGVF forecasting (Muste et al., 2019; 2022a; 2022b).

In this paper, we refer to the HQRC, IVRC, and CSA approaches as conventional methods because they are well established, extensively tested, and thoroughly documented in the literature (Kennedy, 1984 for HQRC; Levesque & Oberg, 2012 for IVRC; Smith et al., 2010 for CSA). The discussion that follows assumes that readers are familiar with the basic principles and procedures of these methods; therefore, they are not reviewed in detail. Instead, we focus on the methodological features most relevant to the present discussion and to the comparison with the proposed HyGage framework.

The century-old HQRC approach remains the predominant method for streamflow monitoring worldwide. In essence, HQRC development relies on an indirect, semi-empirical procedure in which concurrent measurements of discharge and Water Surface Elevation (WSE) are paired to establish a WSE-discharge relationship (Kennedy, 1984). The resulting rating is then refined using statistical methods, some of which have limited physical justification, and supplemented by expert judgment (Fenton, 2018; Rozos et al., 2022). Once established, the rating is used to convert continuously measured WSE (a.k.a. stage) data into real-time discharge estimates.

The IVRC method is based on establishing a relationship between the index velocity ($\boldsymbol{V}_{\mathbf{index}}$) measured continuously at a point, along a sampling line within the water column, or at the water surface, and concurrent direct discharge measurements. Using the surveyed cross-sectional area, A, at the gaging location, the corresponding mean flow velocity, V, is obtained by dividing the measured discharge by the flow area at the time of each discharge measurement. Analogous to the HQRC approach, a rating relationship between V_{index} and V is then developed from these paired observations using regression-based methods (Levesque & Oberg, 2012). Once established, the rating is used to transform continuous index-velocity measurements into estimates of mean velocity and, subsequently, streamflow.

An alternative approach for establishing the V_{index}–V relationship is based on entropy theory, a general stochastic framework that has been applied to a wide range of hydrological systems (Singh, 2025). Chiu (1988, 1989) first introduced entropy theory to river hydraulics by developing the Chiu's Entropy Method. The method is a probabilistic approach founded on the principle of maximum entropy, in which flow velocity is treated as a random variable and its distribution is derived by maximizing entropy subject to known hydraulic constraints, such as the cross-sectional mean velocity.

A key requirement of CEM is calibration of an entropy-based coefficient, an empirical and non-hydraulic parameter estimated from observations of velocity and discharge at a site. The method performs best when the velocity field exhibits a stable and repeatable structure and when the location of the cross-sectional maximum velocity can be identified reliably. These conditions are not always satisfied in natural rivers, where the maximum velocity may occur below the water surface, exhibit multiple peaks, or shift laterally and vertically in response to secondary currents, channel curvature, vegetation, wind effects, or irregular bathymetry. Despite these limitations, entropy-based approaches provide an attractive alternative to conventional index-velocity rating curves (IVRCs). Numerous studies have shown that they can produce reliable estimates of cross-sectional mean velocity under both normal and high-flow conditions while requiring substantially fewer velocity measurements than traditional methods (Moramarco et al., 2004, 2017).

The CSA method tested by these authors (Muste et al., 2019) builds on the original Slope-Area (SA) approach developed by Dalrymple and Benson (1967) to extend HQRC ratings to high-flow conditions. In the SA formulation, the bed slope (S_0) in Manning's equation is replaced by the free-surface slope (FSS), while the Manning roughness coefficient (n) is an empirical parameter. By deploying pressure sensors at multiple locations along a stream reach (typically a minimum of three stations), the CSA method enables continuous estimation of the free-surface slope. The method is most effective when applied to relatively short river reaches, typically less than five channel widths in length. Longer reaches may encompass natural hydraulic and geomorphic variations, such as bed-slope transitions, channel bends, or tributary inflows, which can bias free-surface slope estimates and introduce significant discharge errors (Schmidt & Garcia, 2003; House et al., 2025b).

Similar to the IVRC approach, CSA requires a surveyed channel cross section, allowing the cross-sectional area to be estimated dynamically from continuous WSE measurements. The approach has been successfully applied to both steady and unsteady flows in small streams (Lee et al., 2017; Muste et al., 2019) and large rivers (Muste et al., 2025a). While not directly related to CSA needs, it should be mentioned that the FSS measurements gain increased attention in reverse flood routing during normal (Aricò et al., 2009) and extreme events such as flash floods (Spada et al., 2017; Tayfur & Moramarco, 2022). Notable, currently the CSA method is approached with FSS measurements from remote sensing (Bauer-Gottwein et al., 2024; Schwatke et al., 2024; Wang et al., 2025) which is also relevant for implementation of the HyGage method.

The central paradigm shift introduced by the HyGage method is the direct use of the **Saint-Venant Equations (SVE)** to monitor both steady, uniform flows and UGVFs, rather than relying on the semi-empirical relationships and quasi-steady flow assumptions that underpin conventional. The SVE have repeatedly demonstrated their ability to accurately represent UGVF dynamics, even under conditions involving modest channel morphological changes (Litrico & Fromion, 2009; Yu et al., 2020).

Effective implementation of HyGage requires that field conditions reasonably satisfy the assumptions underlying the SVE. Notably, these assumptions generally coincide with the best-practice criteria used for selecting gaging-station locations (Table 1). This overlap highlights a fundamental commonality among all streamflow-monitoring methods: the preference for sites where flow conditions are as simple and free from hydraulic disturbances as possible. A second commonality HQRC, IVRC, and HyGage methods can be implemented using diverse sensing technologies and deployment configurations.

Table 1. Mapping SVE assumptions onto guidelines for selecting gaging sites

Saint-Venant Equations (Saint-Venant, 1871)	**Recommendations for gaging site selection (Rantz et al., 1982)**
Incompressible and constant density fluid. External forces acting on the control volume: pressure, gravity, and frictional resistance. Boundary friction & turbulence accounted for through empirical resistance laws (e.g., Manning, Chezy).	Acceptable for natural rivers.
Hydrostatic pressure distribution applies (small/negligible streamline curvatures and vertical acceleration). No sudden cross-section changes within control volume (CV).	No large areas of scour or fill on stream bed (channel bed quasi- straight)
One-dimensional flow for an infinitesimal channel length (velocity is uniform over the cross section & the water level across the section is horizontal).	Strait stream reach for ∼ 100m
	The gage site is far from confluence with another stream or from tidal effect (to avoid any influence in the gaging site).
Negligible lateral inflow/outflows in the control volume	The total flow is confined to one channel at all stages, and no flow bypasses the site as subsurface flow.
Channel geometry can be represented by cross-sectional averages over the control volume (no overbank flows)	Banks are permanent, high enough to contain floods, and are free of aquatic vegetation or brush
	A satisfactory reach for measuring discharge at all stages is available within reasonable proximity of the gage site (practical concern allowing to make discharge measurements at convenient location).
	Permanent natural or man-made flow controls
The average channel bed is constant and small within CV.	Implicit for most rivers as $S_0 \ll 1$
Flow depth (h) small compared to flood wavelength (L)	Implicit for fluvial wave propagation as shallow water flows are when $h/L \ll 1$)

HyGage Monitoring Concept

The HyGage method presented in this paper is a physically based streamflow-monitoring approach founded on the Saint-Venant equations (SVE). It leverages decades of advances in streamflow observation, integrating diverse measurement technologies and monitoring concepts into a unified framework. By directly incorporating the governing equations of open-channel flow, HyGage moves beyond empirical rating-based approaches and exploits the increasing availability of high-resolution hydraulic measurements to provide more physically consistent estimates under both steady and unsteady flow conditions.

An intuitive form of the SVE for monitoring purposes is its non-conservative version provided by Eq. (1) that relates the steady uniform discharge, Q_0, (obtained herein via Manning equation) with the unsteady, non-uniform discharge, Q, stemming from various UGVF regimes (e.g., Henderson, 1966):

$$Q = Q_0 \sqrt{1 - \frac{1}{S_0}\frac{\partial h}{\partial x} - \frac{V}{gS_0}\frac{\partial V}{\partial x} - \frac{1}{gS_0}\frac{\partial V}{\partial t}} \quad (1)$$

[steady uniform ---→]
[steady non-uniform (gradually varied) ----------→]
[unsteady non-uniform (spatial-temporal gradually varied) →]

where variables h (depth) and V (cross-sectional velocity). The number of terms on the right side of SVE is associated with the type of fluvial wave propagating through the observation point (Henderson, 1966): kinematic (first term), diffusive (first three terms), fully dynamic (all terms). More specifically, the kinematic wave accounts only for friction and gravity forces, the diffusive wave appends the pressure force, while the fully dynamic wave also includes the local acceleration forces. The SVE inherently accounts for local morphological changes through the pressure-gradient and convective terms in Eq. (1).

The change in signs of the variable derivatives on the rising and falling limbs of the hydrograph in Eq. (1) leads to hysteretic (non-unique) relationships between any pair of UGVF hydraulic variables (i.e., *FSS*, *V*, and *WSE*). The departure of these hysteretic relationships from the unique HQRC function for steady and uniform flow (Q_0) are visualized as loops in the relationships between pairs of hydraulic variables and phase lags between the peaks of the variable hydrographs (Muste et al., 2025a). The variable peak phasing progresses strictly in the following order: *FSS*, *V*, *Q*, and *WSE*. The hysteresis severity (indicated by the degree of departure of the non-unique relationships from the unique rating curves) is different for each site and propagating event. Broadly speaking, while hysteresis is intrinsically present in all forms of UGVFs, its severity can be mainly related to (Moussa & Bocquillon, 1996; Ferrick, 1985; Perumal et al., 2004; Moramarco et al., 2008; Perret et al., 2022):

- Channel bed slope (low slopes are often leading to severe hysteresis)
- Flow magnitude and flashiness (high, sharp hydrographs produce severe hysteresis).
- Froude # (for $\mathrm{Fr} \ll 1$ severe hysteresis; for $\mathrm{Fr} < 1$ moderate, and for $\mathrm{Fr} > 1$, negligible).

Directly determining discharge with Eq. (1) requires continuous direct measurements of the primitive hydraulic variables h and V and of the spatial-temporal gradients appearing in the last three terms of the equation. The flow depth, h, is usually derived from the measurement of stage (WSE). The WSE value is not necessarily zero when the effective flow depth is zero. The derivative $(\partial h/\partial x)$ is mathematically equivalent to FSS estimated over a distance commensurate with the wavelength of the propagating fluvial wave (House et al., 2025a). Selecting longer river reach lengths departs from the scales of the SVE discretization that are strictly valid for elementary flow volumes. We deem that, similar to Petersen-Øverleir (2006) finding, the HyGage monitoring concept is applicable for situations where changes in channel geometry and resistance are relatively small during UGVFs, i.e., of the same order of magnitude as the discharge measurement uncertainty. If this is not the case, further segmentation is needed over time-periods and space-intervals when the flow control can be considered closer to stable (House et al., 2025a).

One of the most difficult tasks in applying Eq. (1) in practice is to determine FSS over short distances in the vicinity of the station because its estimation depends on instrument resolution and accuracy, as well as on the bed slope and event magnitude (e.g., WSDOT, 2025). However, studies showed that modern instruments are capable to capture free-surface slopes over distances as small as tenth of meters (Smith et al. 2010; Muste et al. 2025b). Another difficult task is to analytically convert the index velocity (V_{index}) into bulk flow velocity (V) instead of using empirical ratings as currently done for IVRC method. This task is still under research, with some successful attempts demonstrated in prior works (Le Coz et al., 2008; Nihei & Kimizu, 2008: Hoitink et al. 2018; Johnson & Cohen, 2017; and Fenton, 2025). In this paper we tackle the V_{index} to V conversion with the entropy concept, discussed in the previous section and implemented using dedicated software developed by our team (Kim et al., 2025). Overcoming the above-mentioned difficulties allows for application of Eq. (1) fully analytically without additional restrictive assumptions.

In order to demonstrate the impact of directly measuring all or only some of the terms in the SVE to capture the actual UGVF features, we made recourse to numerical simulations carried out with 1-D unsteady HEC-RAS applied to a hysteretic site investigated through several prior studies (Muste et al., 2022a, 2022b; House et al., 2025a, 2025b; Muste et al, 2025a). Fig. 1 replicates hysteretic features simulated for a large flood wave propagating through a 300m-long reach downstream from the USGS station # 0555830 at Henry on Illinois River (IL, USA). The event simulation allows to readily represent the discharge time series, labeled Q_{HyGage} (Dyn), accounting for all the SVE terms in Eq. (1) - similar to what HyGage would measure - as well as discharges provided by a hypothetical CSA monitoring, Q_{CSA} (Diff), obtained by retaining only the $\partial h/\partial x$ term in the summation. The plots in Fig. 1 also contain datasets provided by the IVRC method, Q_{IVRC} (semi-empirical), as reported by USGS who maintains and operates IVRC at this site. The switch from a prior HQRC, labeled Q_{HQRC} (Q_0), to IVRC for this site was triggered by repeated instances when flow measurements with the HQRC method were deemed inaccurate.

Finally, Fig. 1 includes the HQRC discharge series corrected using the Fread (1975) algorithm, Q_{FRE}(applied to Q_0), to illustrate the performance of a representative HQRC unsteadiness-correction method (see Muste et al., 2025b, for a broader evaluation of HQRC correction approaches). This method is included here because it is also used in the HyGage comparison at the Clear Creek site, where numerical-simulation results are unavailable. The Fread method is particularly attractive because it is parsimonious, requiring only water-surface elevation (WSE) measurements at a single location together with a hydraulic correction derived from the Saint-Venant equations. Previous studies have shown that the method can accurately reproduce hysteretic stage-discharge relationships. It has been further refined by Lee and Muste (2017) and has recently been incorporated into USGS software applications (Domanski et al., 2025).

Given that there are no direct discharge measurements for this 1.5-month event (a daunting task itself), we cannot conclude on the most reliable of the five methods illustrated in Fig. 1. However, relatively speaking, it is apparent that the hysteretic loops and the time series offered by the simulated HyGage and CSA methods are in close agreement while the HQRC datasets corrected with the Fread method and the IVRC datasets are slightly off. It is quite apparent that the simple stage-discharge (HQRC) method completely overlooks the dynamics of the flow propagation. Numerical simulations replicating this event illustrate that the uncertainty in the HQRC discharge can reach significant differences from the actual flows in the area of the maximum loop size for same stages on the rising and falling limbs of the hydrograph. Also notable is that discharge hydrographs for the HyGage, CSA, IVRC and Fread methods plotted in Fig. 1 are peaking at higher values and occur prior to the timing of the discharge peak of the HQRC. The hysteretic features illustrated in Fig. 1 are akin to those found through multiple prior studies at a variety of sites conducted by these authors (Muste et al., 2025a; 2025b).

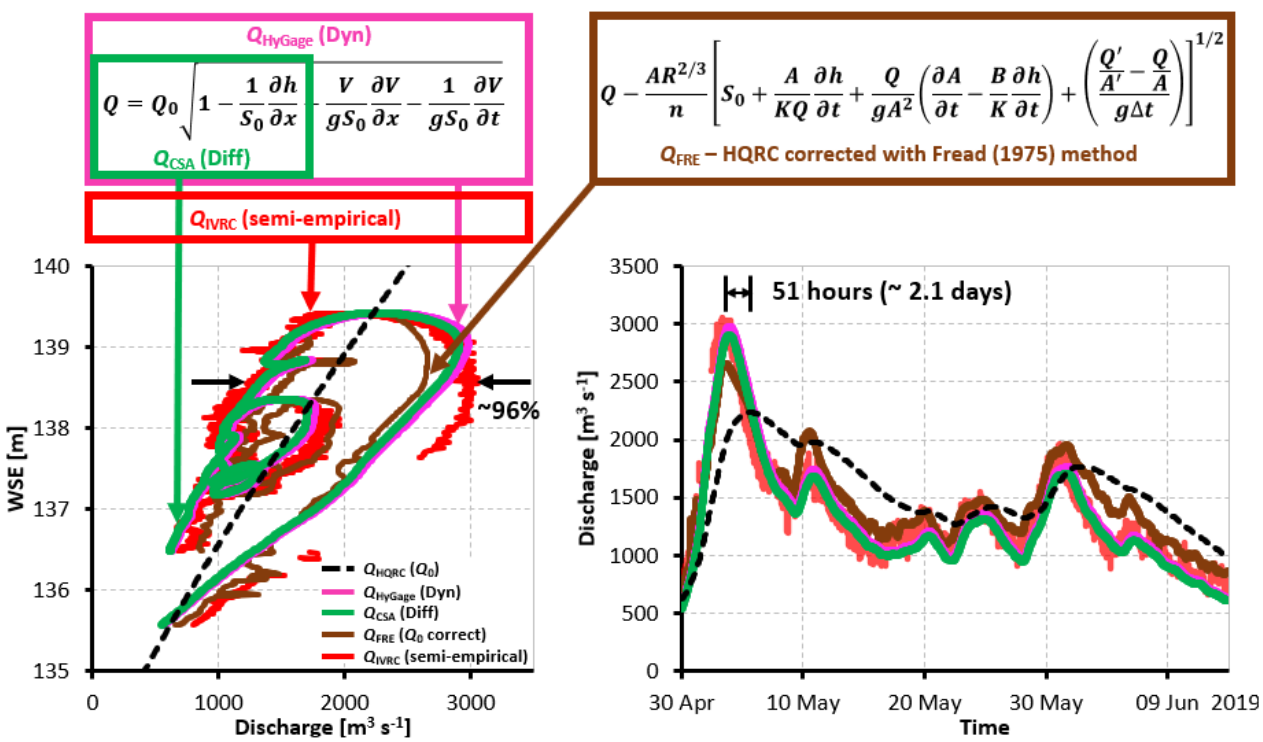

Figure 1. Comparison of the tracing of hysteretic features provided by various streamflow monitoring approaches.

EXPERIMENTAL RESULTS

Test site

The Oxford site is closely located with an HQRC operational station (USGS #05454220) installed 214 m upstream from the center of the HyGage test section (see Tab. 2). Essential specifications for the Oxford test site on Clear Creek (Iowa) are also shown in Tab. 2. The selection of this site followed a careful evaluation of their ability to satisfactorily meet the constraints inherent in the SVE (see Table 1). In particular, the gaging location exhibits quasi-prismatic and relatively straight channel geometry in the vicinity of the station, a cross-section that remains stable over time, well-defined channel control at the measurement site, and minimal to no backwater influence. These characteristics collectively ensure that the underlying hydraulic assumptions of the governing equations are reasonably satisfied, thereby supporting reliable application of the monitoring methods under investigation. Prior studies revealed the stability and repeatability of the measurements with various methods applied to this site (Lee et al., 2017).

Table 2. Hydraulic specifications for the test station analyzed in this study

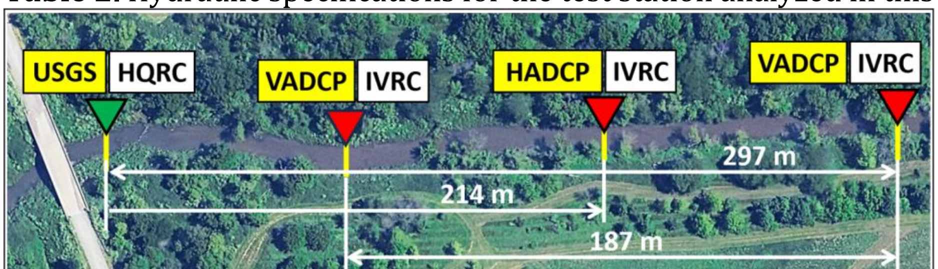

Station equipment	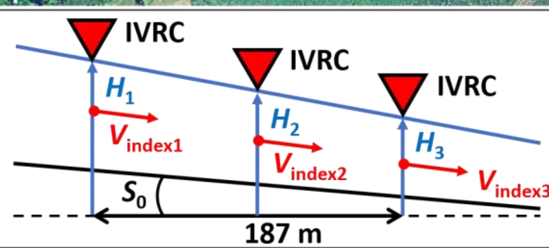
S_0	**0.00039**
Base *n*	**0.025**
***B* [m]**	**10**
B/h	**15**
$Q_{min - max}$ [m^3 s^{-1}]	**≈ 1.3 – 25**
$Q_{annual\ mean}$ [m^3 s^{-1}]	**46**
Fr	**0.161 – 0.236**
Drainage area [km^2]	**151**

HyGage instrumentation layout

Ensuing from the above section, the HyGage monitoring concept combines measurement elements pertaining to IVRC (i.e., cross-section area and an index velocity) and CSA (i.e., cross-section area, FSS, and Manning's *n*) methods. Specifically, the HyGage relies on experimental procedures that provide the mean flow velocity (via V_{index}) and the free-surface slope (FSS). There is a myriad of instruments available for acquiring these variables in real time including in-situ submersed or close- and remote-sensing technologies (Tsubaki et al., 2025). In this paper, we present the first published account of implementing the HyGage method at a full-scale, operational gaging station.

For the Oxford HyGage test site, we deployed a horizontal Acoustic-Doppler Current Profiler (HADCP) and two Vertical ADCPs (VADCP) as schematically illustrated in Figure 2. The HADCP measures velocities across a line in the channel, while VADCPs measure velocities in verticals centered on the instrument axis. The free-surface elevations were measured with pressure sensors embedded in the ADCP units and with an independent bubbler in the central section of the test reach. The Oxford site has been intentionally over-instrumented to enable various redundant measurements for supporting the testing and validation of the HyGage protocols targeted through Muste et al. (2023) study. Notable, two HADCPs deployed in Sections 1 and 3 would suffice to ensure that the hydraulic variable and their gradients are readily available for HyGage implementation.

Similarly to the IVRC and CSA methods, discharge computation with HyGage requires a stage-area relationship to estimate cross-sectional area as a function of water level. To develop this relationship, repeated cross-sectional surveys were conducted at all three sites using either a total station or RTK-GNSS equipment. Regardless of the monitoring approach employed, periodic cross-section surveys are recommended because they enable the detection and documentation of channel morphological changes that may affect stage-discharge or stage-area relationships (Kennedy, 1984).

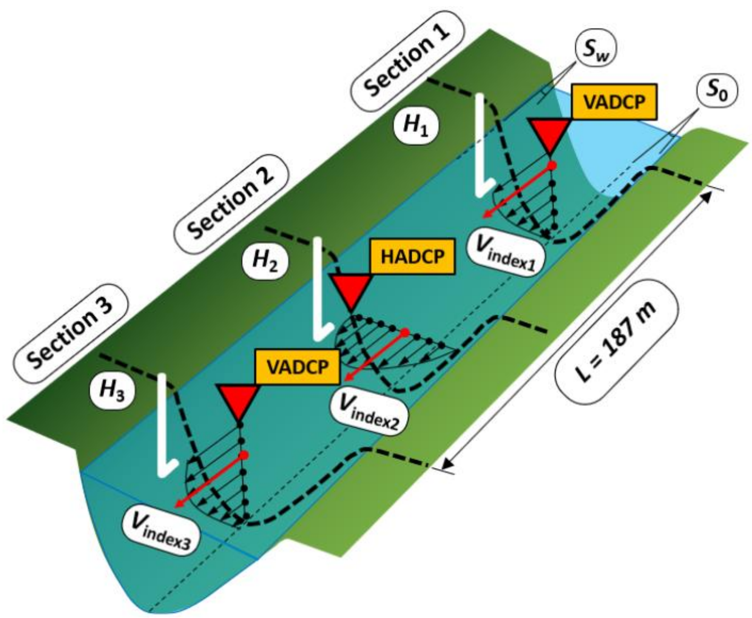

Figure 2. HyGage instrument layout at Oxford test site

Analysis dataset

Because the Oxford test site was instrumented specifically to evaluate the HyGage method, direct measurements of all hydraulic variables and gradients included in Eq. (1) were obtained using state-of-the-art deployment and sampling practices. The highest stage observed during the study period (2020-2024) was 215.4 m. The four events selected for analysis (S#1-S#4 in Figure 3a) have return periods shorter than 15 years, consistent with the prolonged drought conditions that characterized the study period. All event stages remained below the bankfull elevation (Figure 3b). Figure 3c shows the site rating curve derived for Section 2 - the central section of the test reach - using the Fenton (2018) method ($Q_{0\text{-FEN}}$) applied to the complete set of direct discharge measurements available from the USGS station, along with the hydrograph of the largest event reconstructed using the Fread method (Q_{FRE}). The Fenton (2018) method is an automatic computation stage-

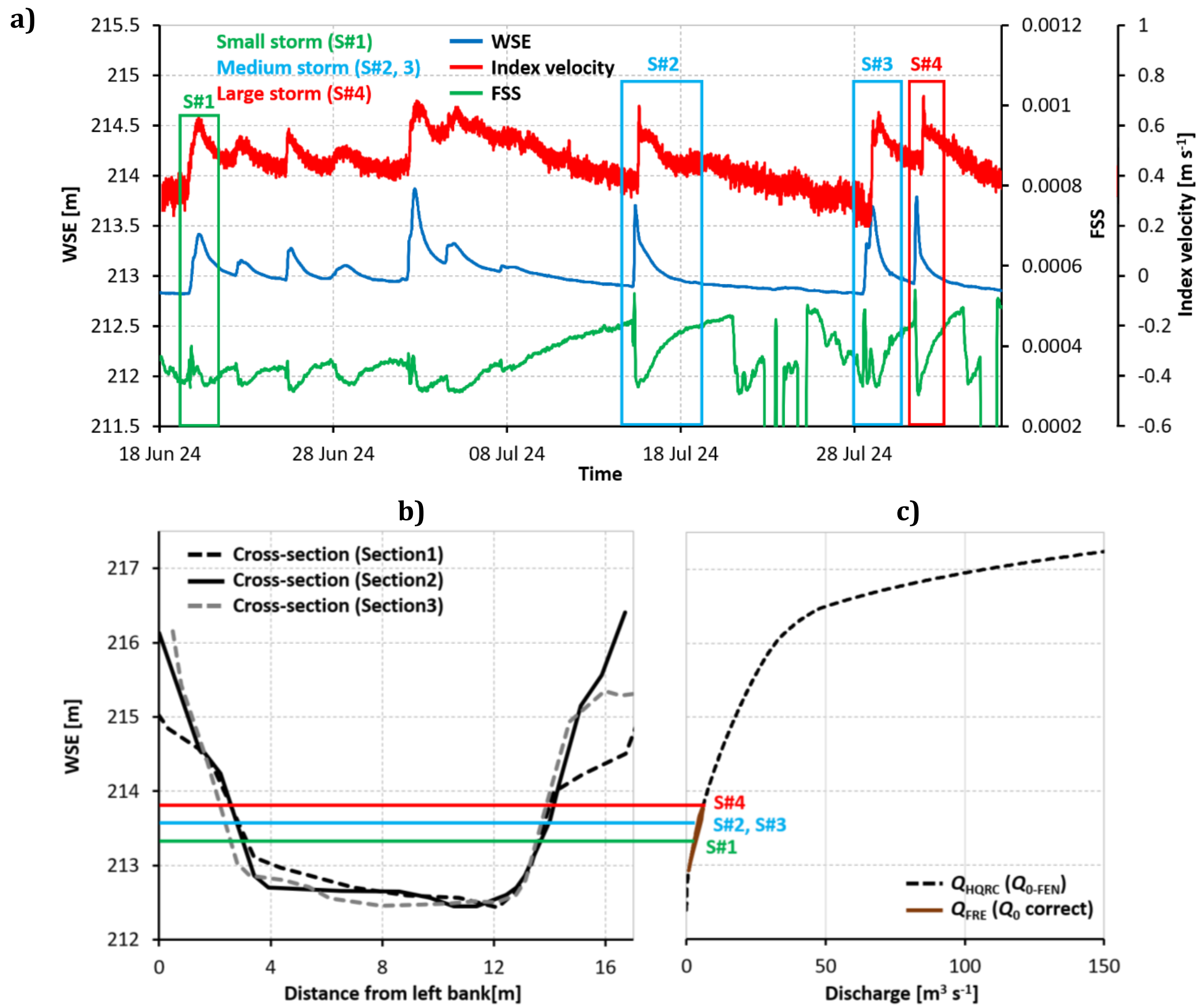

Figure 3. Analysis considerations for the Oxford test site: a) time series for the analyzed hydraulic variables; b) cross-section along with traces of the maximum stages for the two analyzed storm events; and c) the reference HQRC for the site ($Q_{0-\text{FEN}}$) and the trace of the largest storms estimated with Fread method (Q_{FRE}).

During the 2024 deployments, the station was equipped with three ADCPs (two Sontek-IQ Plus VADCPs and a Sontek-SL 1500 HADCP) arranged as illustrated in Figure 2. The VADCPs were located at the end of the test section and the HADCP was installed in the central cross section. The station's instruments were synchronized on the data logger clock to acquire data every 15 minutes and synchronized with the timing of the USGS data collection system. The flows at Oxford test site and in the drainage area leading to the station are free of man-made hydraulic structures. It is worth noting that the flow traces for the two storms shown in Figure 3c do not exhibit readily visible hysteretic behavior. However, when the same events are examined using magnified axes in the subsequent analysis, the expected hysteresis patterns become unmistakably apparent, despite the relatively small magnitude of the 2024 storm events.

Data Analysis

During the 2024 field campaign (Figure 3a), four storm events were selected for analysis. Although the differences in peak stage among these events are relatively small, they were included to evaluate the sensitivity of hysteretic behavior to variations in hydrograph severity and shape. Based on peak stage value, the events were classified as a small storm (S#1), medium storms (S#2 and S#3), and a large storm (S#4). As shown below, storms S#1 and S#3 exhibit multi-pulse hydrographs, whereas storms S#2 and S#4 are single-pulse events. Identification of the single- or multi-pulse storm type is easier to observe in the WSE traces of Figure 4.

A single-pulse hydrograph is characterized by a monotonic stage variation during the rising and falling limbs, while a multi-pulse hydrograph displays short-duration flow disturbances superimposed on either limb. The former reflects runoff entering the stream under a relatively smooth and continuous change in discharge, whereas the latter results from temporal variations in runoff generation, such as fluctuations in rainfall intensity or the influence of tributary inflows along the study reach. Multi-pulse storms are more representative of natural hydrologic conditions and occur more frequently than idealized single-pulse events. Their analysis, however, requires distinct methodological approaches because of the additional complexity introduced by transient flow disturbances (Muste et al., 2022a).

The primitive variables acquired to implement the full-fledged HyGage methodology for the first three storms are shown in Fig. 4. The raw values for the variables plotted in this figure and the spatiotemporal gradients necessary for HyGage implementation were acquired as follows (see also Fig. 2 and Tab. 2 for instrumentation arrangement): V_{index} was measured with the HADCP located in Section 2; FSS time series were determined using the stages recorded by the pressure sensors embedded in the two VADCP located 187-m apart in the terminal sections of the test reach Sections 1 and 3 (see Figure 2). Stream stages (WSE) were measured with the pressure sensor located in the HADCP unit. An additional independent pressure sensor collocated with the HADCP was used for backing up data in equipment failure situations.

The time-series plots in Figure 4 are shown in non-dimensional coordinates by normalizing each variable with its event-specific maximum value. This scaling highlights the hydrograph peak sequencing, which consistently follows the order FSS → V (V_{index}) → WSE. Overall, the observed sequence agrees with the numerical simulation results presented in Figure 1. Two aspects of the time series shown in Figure 4 warrant further attention. First, the time lags between successive peaks are substantially smaller than those observed in

Figure 1. This difference reflects the contrasting scales of the two study rivers. Clear Creek is a small, wadable stream with an aspect ratio of approximately 15, whereas the Illinois River has an aspect ratio of about 80 (Muste et al., 2022b). Consequently, Clear Creek exhibits a faster hydraulic response and shorter peak-to-peak lag times. The second aspect is specific to event S#1 and is manifested in the FSS record along the rising limb of the hydrograph. This feature is associated with a particular measurement condition encountered during data collection and is discussed in detail in the Discussion section.

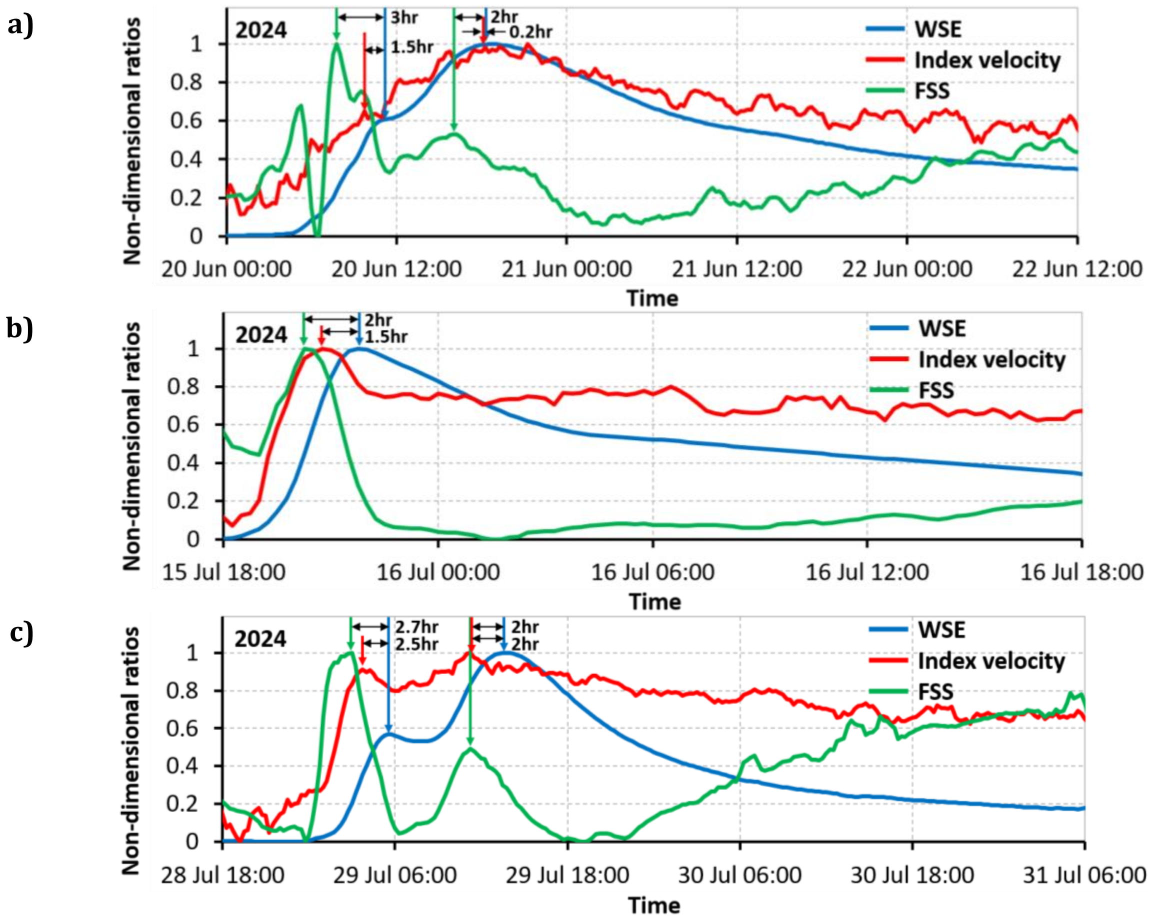

Figure 4. Hysteretic relationships in the time series of the measured variables for storms: a) S#1; b) S#2: and S#3.

The effects of storm magnitude and hydrograph type on the stage-discharge relationships and discharge time series obtained using the methods described in Section 2 are illustrated in Figure 5 for storms S#1, S#2, and S#3. The HQRC discharges were estimated using the Fenton (2018) method, whereas the IVRC and CSA discharges were derived following the procedures outlined in the Methods section. The HyGage discharge (Q_{HyGage}) was computed by directly substituting the measured hydraulic variables WSE, V, and FSS into Eq. (1). Figure 5 also includes the discharge series Q_{FRE}, which seeks to recover the dynamic component of the flow by analytically correcting the HQRC estimates using terms that account for the passage of a fully dynamic fluvial wave through the measurement section.

Conversion of V_{index} to cross-sectional mean velocity (V), required by both the IVRC and HyGage methods, was performed using two independent approaches. The first employed the conventional index-velocity procedure, whereby 15-min HADCP measurements were paired with mean velocities inferred from discharges estimated using the Q_{FRE} method applied to the HQRC time series. The second approach used the entropy-based velocity model described in the Methods section. This model requires as input the HADCP velocity records and the cross-sectional geometry surveyed at the instrument location. Calibration and validation of the entropy model were carried out using VADCP measurements collected in end sections of the study reach. Although either dataset could have been used for model development and verification, the selected configuration was considered preferable because the HADCP was installed near the channel bed, where lateral velocity variability was relatively small. In contrast, the velocity profiles obtained with the VADCP provided a more comprehensive representation of the cross-sectional velocity distribution and therefore offered a more robust basis for validation of the entropy model.

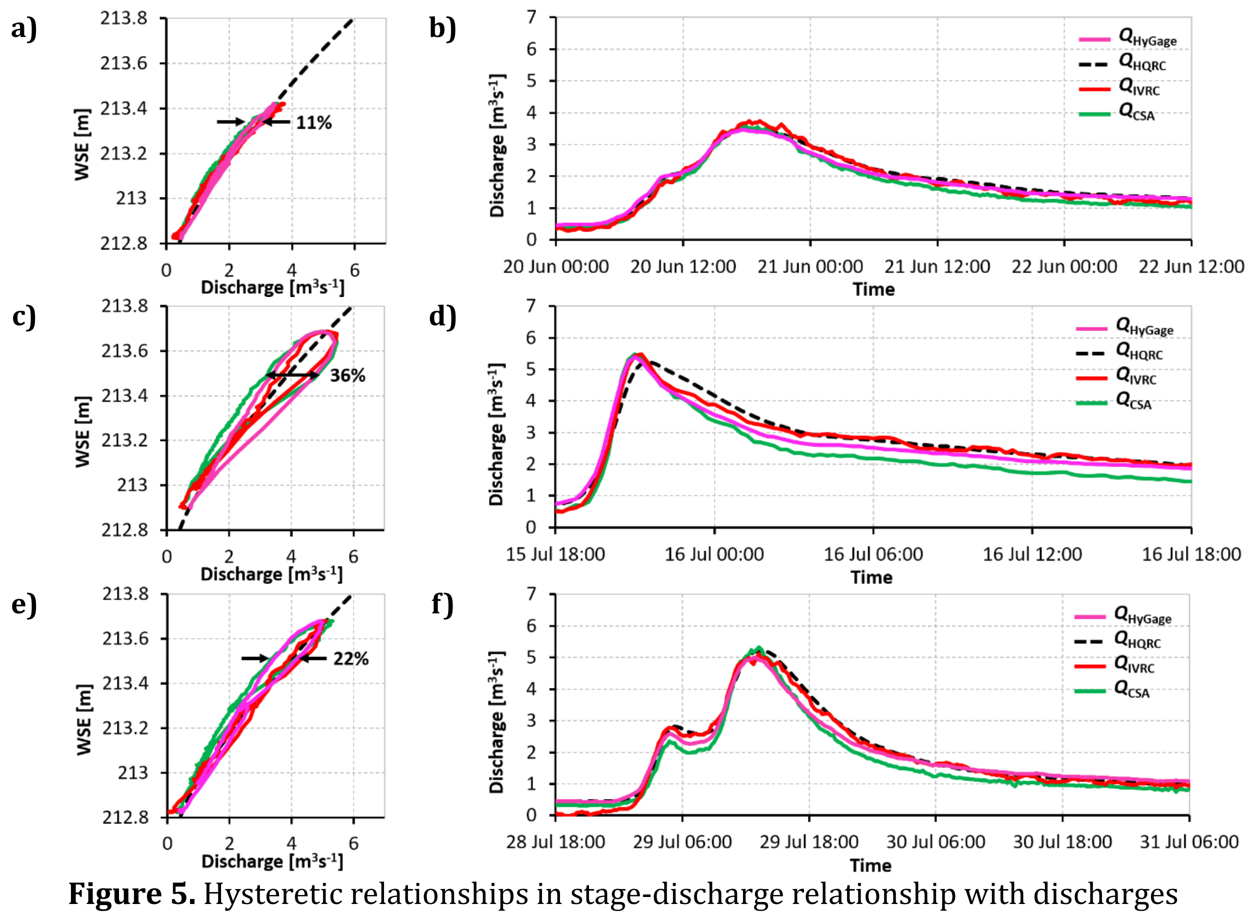

Figure 5. Hysteretic relationships in stage-discharge relationship with discharges estimated with various monitoring methods: looped relationships for storms: a) S#1; c) S#2; and e) S#3; discharge time series for storms: b) S#1; S#2, and S#3.

The discharge estimates obtained using the various monitoring methods, together with the corresponding stage records plotted in both time-independent stage-discharge coordinates and time-dependent discharge graphs, revealing recognizable hysteretic behavior during the first three storm events of 2024 despite the relatively small size of the stream. The maximum widths of the hysteresis loops correspond to approximately 11%, 22%, and 36% of the HQRC discharge for the same stage for events S#1, S#2, and S#3, respectively. These values can be interpreted as an indication of the potential magnitude of uncertainty associated with the conventional HQRC estimates during these events. Although storms S#2 and S#3 reached the same maximum stage (213.7 m), the larger hysteresis loop observed for S#2 is attributed to its more rapid and nearly monotonic stage rise. Indeed, S#2 can be characterized as the flashiest of the first three events because of its steeper rising limb and sharper hydrograph shape, which enhanced unsteady-flow effects.

The discharge time series in Figure 5b show only minor differences among the methods because of the relatively small magnitude of event S#1. In contrast, the larger storms S#2 and S#3 exhibit clearer separation among the discharge estimates, highlighting the earlier response of the HyGage hydrograph and a more pronounced divergence from the other methods, particularly along the falling limb of the hydrograph. It is noteworthy that repeated investigations at this site over the years have produced hysteresis loop sizes and peak-lag relationships consistent with those observed during the 2024 storms (e.g., Lee et al., 2017; Muste et al., 2019), providing further confidence in the reproducibility of the observed hydraulic behavior.

We present the largest storm event recorded during the 2024 deployment separately, not only because it produced the highest stage of the observation period, but also because its single-pulse hydrograph allows direct comparison with generic features identified in previous studies conducted at other sites using the IVRC method (Muste et al., 2022b) and at the same site using the IVRC and CSA method (Muste et al., 2025a). The time series of the directly measured variables shown in Figure 6a illustrates the peak phasing of the hydrograph components in the expected sequence (i.e., FSS, V, and WSE), with lag times comparable to those observed during the first three storm events. In contrast, the looped stage-discharge relationship obtained with the HyGage approach and illustrated in Fig. 6b is considerably enlarged, exhibiting a hysteresis width that is more than twice that observed for the preceding events and departures from the simple HQRC of more than 20%. As demonstrated in previous studies, hysteresis is not limited to the stage-discharge relationship; rather, it reflects a broader non-uniqueness in the relationships between hydraulically coupled variables. This behavior is evident in the WSE–V_{index} and WSE–FSS relationships shown in Figures 6c and 6d, respectively.

Figure 6e compares the discharge time series obtained using all monitoring approaches, including Q_{FRE}, which is used here as a surrogate reference because direct discharge measurements were unavailable throughout the storm-event propagation. The hydrographs demonstrate the inability of the conventional HQRC method to adequately capture the dynamics of unsteady flow conditions, in contrast to the discharges derived from the IVRC, CSA methods, and the HyGage protocols. Notably, the HyGage hydrograph indicates an earlier discharge peak, occurring approximately 0.7 h before the HQRC peak, and a peak discharge that is 2.6% greater than the HQRC estimated value. The more dynamic character of the hysteretic flow captured by IVRC, CSA and HyGage methods relative to the HQRC approach, is clearly reflected by the steeper rising and falling limbs of the corresponding hydrographs.

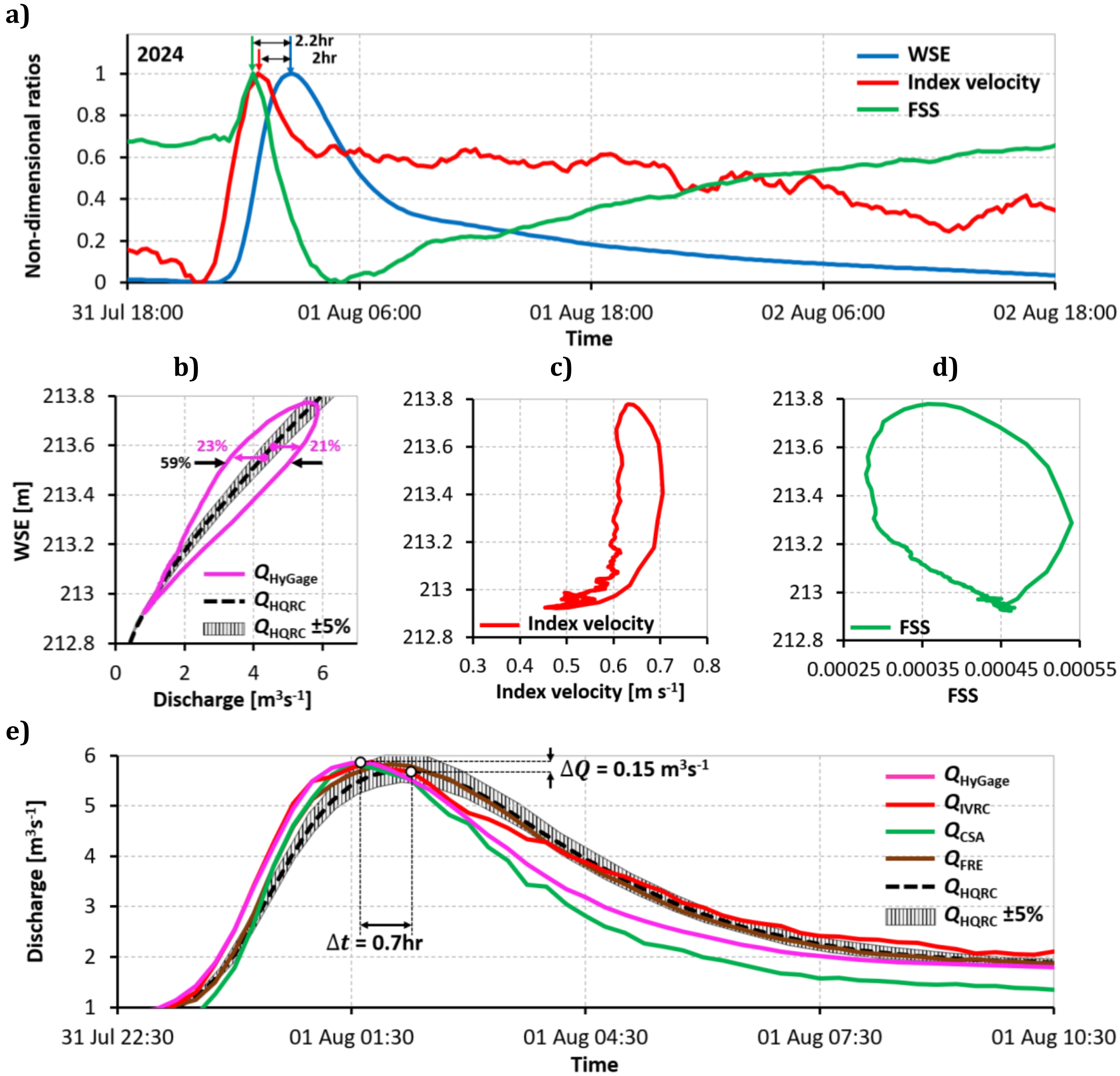

Figure 6. Hysteretic characteristics of the HyGage monitoring protocol during storm event S#4 and comparison with alternative discharge-monitoring approaches, including the conventional HQRC method. a) Time series of directly measured hydraulic variables; b) stage-discharge relationships obtained with the HyGage and HQRC protocols; c, d) hysteretic relationships between WSE and V_{index}, and between WSE and FSS, respectively; (e) discharge hydrographs derived from all monitoring methods investigated.

Although the differences among the monitoring approaches over the full event are of considerable interest, the limited dataset available in this study, together with the absence of ground-truth measurements and/or companion numerical simulations such as those presented in the Methods section (Fig. 1), precludes a robust quantitative evaluation of method performance and associated dataset uncertainties. Nevertheless, comparison with the $\boldsymbol{Q}_{\mathbf{FRE}}$ hydrograph, the only common reference between Figures 1 and 6, indicates generally good agreement with the dynamic monitoring methods as discussed next. With respect to uncertainty, the most defensible approach is to apply a ±5% discharge uncertainty band to the HQRC estimates (Fig. 6e), consistent with the uncertainty commonly attributed by the USGS to well-executed streamflow measurements under near-steady flow conditions (Schmidt, 2002). Within this framework, instances in which HyGage-derived discharges fall outside the HQRC uncertainty bounds may be interpreted as evidence of genuine unsteady-flow and hysteretic effects, rather than as artifacts of measurement uncertainty alone.

DISCUSSION

Consistent with previous analyses conducted at more than 20 gaging sites worldwide (Muste et al., 2022b; 2025b), the results of this study further confirm that actual flow conditions can deviate substantially from those estimated using conventional HQRC method, even at sites characterized by relatively weak hysteresis. It should be emphasized that the Oxford test site was selected primarily because it provided the key datasets required to evaluate the capabilities of the HyGage method, rather than because it experiences pronounced hysteresis during UGVF events. To the authors' knowledge, no other dataset currently exists in which all the monitoring methods and instruments considered herein were operated simultaneously across multiple hydrological events.

Evidence of hysteresis and method comparison. The time-dependent and time-independent relationships among the primary hydraulic variables, namely water-surface elevation (WSE), index velocity (V_{index}), and free-surface slope (FSS), shown in Figures 4 through 6 exhibit the expected signatures of hysteresis (see also Figure 1). In particular, the correspondence between hydrograph peak separation, the magnitude of the looped variable relationships, and the expected progression of these features with the increase in storm intensity clearly reflects hysteretic behavior, even though the observed UGVF events were comparatively mild.

The most notable finding in the present context is that the multivariable relationships presented in Figures 4, 5, and 6 show clear departures of the HyGage, IVRC, and CSA methods from the one-to-one stage-discharge relationship represented by the HQRC during event propagation. In particular, the HyGage measurements demonstrate that hysteresis is event-dependent, as evidenced by the departures ranging from 11% to 59% among the four storm events analyzed (see Figures 5a-c and 6b). This behavior demonstrates that these methods capture dynamic flow characteristics that are inherently missed by conventional HQRC approaches. These deviations can be interpreted as uncertainty bands associated with the epistemic uncertainties in the discharge estimates derived from HQRCs.

Further insights into the intercomparison of the presented monitoring approaches are obtained from an examination of the discharge hydrographs obtained using HQRC and those estimated with the more dynamic HyGage, IVRC, and CSA methods for events S#1, S#2, and S#3 (Figures 5b, 5d, and 5f, respectively) and storm S#4 (Figure 6e). These differences are most readily observed in the single-pulse storm events shown in Figures 5d and 6e. In particular, the dynamic methods (IVRC, CSA, and HyGage) generally anticipate the HQRC response along the rising limb, with HyGage producing discharge estimates that lead those from the other dynamic methods. Along the recession limb, discharge estimates from the dynamic methods are typically lower than those derived using HQRC. Among the dynamic approaches, IVRC shows the closest agreement with HQRC, whereas HyGage and CSA exhibit greater deviations, both from HQRC and from each other. Notably, CSA consistently produces the lowest discharge estimates throughout the recession period.

The FSS hysteresis loop derived from HyGage measurements is noticeably more pronounced than the hysteresis observed in the stage-discharge and stage-index velocity relationships (Figure 6b-d). This finding suggests that hysteretic effects exert a stronger influence on the WSE-FSS relationship, underscoring the value of incorporating FSS measurements at monitoring sites where hysteresis is significant. Similar patterns have been consistently documented in previous studies conducted by the authors across multiple streamgaging locations (Muste et al., 2025a, 2025b), further supporting the robustness and broader applicability of this observation.

The HyGage protocol is instrument-agnostic, offering a key advantage over conventional USGS monitoring approaches, including HQRC, IVRC, and CSA. In other words, the protocol can be implemented using a wide range of submerged, near-surface, and remote-sensing instruments for measuring stage and index velocity. The core HyGage protocol applied in this study relies on direct measurements of WSE, index velocity (V_{index}), and FSS, combined with an embedded entropy-based model that converts index velocity into cross-sectional mean velocity. Unlike traditional stage-discharge or index-velocity rating approaches, this methodology does not depend on rating curves and therefore avoids the need for extrapolation beyond the range of observed conditions. The entropy model is highly adaptable and can utilize various forms of index velocity measurements, including radar-derived point velocities, image velocimetry applied to the free surface, and data from vertical or horizontal acoustic velocity profilers, requiring only minimal adjustments and substantially fewer calibration measurements than either HQRC or IVRC methods.

From an operational perspective, the HyGage system described in this study is capable of generating discharge estimates using data collected over sampling periods shorter than 3 minutes. This sampling interval is approximately one-fifth of the 15-minute interval commonly employed throughout the USGS streamgaging network. Consequently, the HyGage protocol offers greater flexibility and responsiveness than conventional methods, particularly for flash-flood applications where water levels may rise to the flood crest within less than six hours. Furthermore, flood waves associated with flash floods are often predominantly kinematic in nature, which further simplifies the measurement requirements by reducing the number of direct observations needed to estimate discharge reliably. These characteristics suggest that the HyGage protocol is particularly well suited for monitoring rapidly varying flow conditions where traditional rating-based approaches may face significant operational limitations.

The presented results indicate that the HyGage method can perform reliably even under less-than-ideal hydrologic and logistical conditions, provided that the gaging site is appropriately selected. Successful application of the method depends on careful site selection, including compliance with the criteria outlined in Table 1, as well as the use of suitable instrumentation and measurement protocols with spatial and temporal resolutions commensurate with the scale and propagation characteristics of the flood wave. These factors are critical for isolating hysteretic effects from other hydrogeomorphic processes that may influence flow dynamics and obscure interpretation of the observed relationships.

Methodological limitation and uncertainty. The resources available for the present investigation did not allow for the collection of extensive independent discharge measurements during UGVF events, resulting in a lack of ground-truth data for direct evaluation of the tested methods and the development of site-specific datasets required for a rigorous uncertainty analysis (UA). Consequently, a comprehensive assessment of method performance and associated uncertainties could not be undertaken within the scope of this study. Benchmark datasets with sufficient temporal resolution for this type of analysis are rare (e.g., Faye & Cherry, 1980 with older generation instrumentation), largely because of the substantial logistical and financial resources required to obtain them. In addition, the periods for which complete HyGage observations were available at the Oxford site did not encompass a broad spectrum of UGVF events, restricting the opportunity to assess method performance under varying degrees of hysteresis.

Beyond the financial and hydrological constraints encountered in this study, additional technical challenges limited the acquisition of suitable ground-truth data at the study site. A rigorous uncertainty assessment would require repeated direct discharge measurements throughout the passage of individual flood waves. For the study reach, the most reliable conventional approaches are ADV-based wading measurements during low-flow conditions and ADCP transects during higher flows. However, obtaining a single verification measurement requires approximately one hour using ADV and at least 30 minutes using ADCP, even when employing rapid, lower-quality survey protocols. Over such time intervals, the assumption of steady flow is untenable, as evidenced by the continuously varying stage records observed during the monitored events. Moreover, ADV measurements become increasingly hazardous during elevated flows, while ADCP measurements conducted under highly unsteady and sediment-laden flood conditions are themselves subject to considerable uncertainty and operational limitations.

Practical Implementation Issues. The datasets analyzed herein provide valuable practical insights into the implementation of both HyGage as well as of the conventional IVRC method, which, aside from the stage-discharge rating curve (HQRC), remains the most mature and widely adopted discharge-monitoring approach in the United States. One issue that warrants further investigation is the reliability and representativeness of index velocities measured with horizontal HADCPs. These instruments typically sample velocities along an acoustic path that often spans only a fraction of the river width, even during low-flow conditions. In this regard, Hoitink (2018) notes that a side-looking HADCP should ideally extend beyond the distance from the bank at which the depth-averaged velocity exceeds the cross-sectional mean velocity, a requirement that is difficult to satisfy in large rivers characterized by pronounced cross-sectional variability.

Furthermore, the physical relevance of sampling velocity distributions along HADCP lines of sight may be questioned when compared with measurements collected along vertical profiles located within the deeper portions of the channel. Flow-field distortions associated with secondary currents and other three-dimensional hydraulic features can significantly affect the reconstruction of the cross-sectional velocity distribution from a limited horizontal sampling domain. Such effects may be more detrimental than those associated with measuring a representative vertical velocity profile and subsequently extrapolating it across the river width, as commonly practiced in velocity-index methods (Le Coz et al., 2008). Finally, the persistent inability of some HADCPs to measure velocities in the far-field portion of the acoustic path remains an important operational challenge. Addressing this issue requires first identifying the underlying cause, such as reduced acoustic signal return, and then developing robust correction procedures supported by a limited number of targeted field-verification measurements.

The introduction and testing of the entropy model as a substitute for the conventional V_{index}–V conversion procedure used in IVRC applications has also proven beneficial for HyGage. Compared with the labor-intensive development and maintenance of traditional IVRC relationships, the entropy-based approach offers a more parsimonious and physically grounded alternative. In the present study, index velocities (V_{index}) were measured along a horizontal acoustic path and subsequently transformed into estimates of cross-sectional mean velocity (V) using a relatively small set of input data. The entropy framework offers substantial flexibility because it can accommodate velocity observations acquired at a point, along a vertical or horizontal profile, or over larger portions of the flow field. In addition, its computational efficiency makes real-time implementation feasible. Another advantage of the entropy model is that it enables the computation of discharge (Q) through analytical formulations rather than reliance on empirical correlations between measured variables, such as V_{index} and Q, whose statistical relationships do not always explicitly represent the governing flow physics. Recent studies indicate a growing adoption of entropy-based approaches as alternatives to conventional IVRC methodologies across a range of index-velocity measurement configurations (e.g., Moramarco et al., 2019; Bahmanpouri et al., 2022; Kechnit et al., 2024; Singh, 2025).

A close examination of the FSS time series presented in Figures 4 and 6a reveals a characteristic depression immediately following the FSS peak, which consistently occurs before the WSE peak. This behavior indicates that the spacing between the stage sensors falls within the optimal range for accurately capturing hysteretic UGVF dynamics, as demonstrated through numerical simulations by House et al. (2025a). The observed FSS trends further show that the FSS peak occurs near the inflection points of both the rising and falling limbs of the WSE hydrograph, a behavior previously documented by Rátky (2000) and Muste et al. (2025a). Identifying these characteristic points in hydraulic-variable time series provides a valuable means of assessing the adequacy and robustness of monitoring-system layouts and data-acquisition protocols.

One unexpected feature evident in the FSS records shown in Figures 4 and 6a is the pronounced fluctuation observed along the rising limb of event S#1. Although the use of nondimensional scaling exaggerates the visual prominence of this perturbation relative to the other hydraulic variables, an additional factor appears to contribute to the anomaly. The FSS is computed from stage measurements acquired at Sections 1 and 3, and a closer inspection of the raw stage records indicates that the downstream sensor located in Section 3 registered a temporary departure from the otherwise monotonic stage trend. Specifically, the recorded stage was elevated by approximately 1 cm for a period of about two hours, coinciding precisely with the timing of the anomalous FSS fluctuation. Given that the event produced a total stage variation exceeding 0.6 m above base-flow conditions, the most plausible explanation is that the downstream sensor was temporarily affected by floating debris triggered by the wave inception, which was subsequently removed as water levels continued to rise.

Although minor, this anomaly highlights the importance of accurately measuring small water-surface falls over relatively short channel distances when estimating FSS, a challenge long recognized in slope-based discharge measurements (Dalrymple & Benson, 1967). At the same time, the event serves as a useful reminder of the sensitivity of FSS-based monitoring systems to seemingly small measurement errors. Fortunately, recent advances in noncontact stage-sensing technologies, including high-precision radar- and lidar-based instruments, provide new opportunities for acquiring high-quality water-level observations suitable for reliable FSS estimation (Tsubaki et al., 2025). Such developments are expected to further improve the accuracy and robustness of CSA- and HyGage-based discharge-monitoring applications.

Because the implementation and long-term operation of continuous in situ streamflow-monitoring systems involve significant financial commitments, decisions regarding the adoption of dynamic rating methods should be based on rigorous evaluations of site-specific hydraulic, geomorphic, and hydrologic characteristics, coupled with comprehensive cost-benefit analyses, as discussed by Muste et al. (2025b). Table 3 provides approximate cost estimates for the implementation of IVRC, CSA, and HyGage systems (USGS, 2024, personal communication). However, actual costs can vary considerably depending on factors such as the existing monitoring infrastructure at the site (e.g., upgrades to an existing gage versus installation of a new station), the accuracy and sophistication of the selected instrumentation, and the intended function of the gaging station, whether for routine monitoring, water-resource management, flood forecasting, or hazard-warning applications. Consequently, the selection of a monitoring strategy should balance anticipated accuracy gains against operational complexity and lifecycle costs while accounting for the level of hysteresis expected at the site.

Table 3. Comparative analysis of the costs for various types of monitoring approaches*

Method	HQRC	IVRC	CSA	HyGage
Cost referenced to HQRC (%)	reference	+15	+26	+43

*Cost estimations include operation and maintenance and are instrument- and method-dependent

Future deployment and broader implications. A promising avenue for advancing HyGage implementation is the growing capability to estimate key hydraulic variables in large rivers using remote-sensing technologies that require little or no in situ infrastructure. Notable examples include satellite-based measurements of river water-surface elevation, width, and slope provided through the Surface Water and Ocean Topography (SWOT) mission (Andreadis et al., 2025), as well as emerging efforts to estimate free-surface velocity from space using the Fluvial Video from Satellite (FluViSat) initiative. Similarly, the estimation of free-surface slope (FSS) at regional and continental scales is receiving increasing attention through the application of satellite-borne sensors and related remote-sensing approaches (Sichangi et al., 2018; Bauer-Gottwein et al., 2024; Dhote et al., 2025; Wang et al., 2025). Continued advances in these hydrometric technologies create new opportunities to integrate HyGage with more cost-effective and spatially extensive monitoring systems. Beyond reducing instrumentation and maintenance requirements, remote-sensing observations could expand HyGage from a site-specific gaging tool to a distributed monitoring framework capable of simultaneously supporting multiple river reaches across a watershed with only marginal increases in infrastructure costs. Such developments have the potential to substantially enhance the scalability and operational efficiency of dynamic streamflow monitoring.

In addition to improving streamflow estimation during UGVFs while maintaining effectiveness under steady flows, HyGage offers promising opportunities for advancing hydrologic monitoring, hydraulic modeling, and fundamental research on complex river processes. Beyond discharge estimation, HyGage provides simultaneous observations of key hydraulic variables that can reveal flow dynamics and hysteretic behavior not captured by conventional stage-discharge rating curves. Previous studies have identified several potentially valuable attributes of dynamic-rating-curve data that remain insufficiently explored (Perumal et al., 2004; Dottori et al., 2009). Table 4 summarizes hydrologic, hydraulic, and hydrometric applications that can benefit from HyGage-derived data, highlighting its potential to support improved river monitoring, modeling, and forecasting.

At present, limited evidence exists regarding the relative importance of the three principal drivers of hysteresis: channel-bed slope, hydrograph flashiness, and the Froude number of the propagating wave. Existing analytical insights remain sparse and have yet to be comprehensively validated through experimental observations. Nevertheless, available studies broadly suggest that channel-bed slope may be the dominant controlling factor. For example, Dottori et al. (2009) proposed that rivers with bed slopes (S_0) smaller than $5 \times 10^{-4}$are likely to exhibit hysteretic behavior, whereas Fread (1975) suggested a more restrictive threshold of 1×10^{-4}. Similarly, Perumal et al. (2004) developed the $|(1/S_0)\, \partial h \,/\, \partial x| \leq\ 0.5$) criteria for distinguishing between kinematic and diffusive wave propagation, thereby providing a framework for assessing the likelihood of hysteresis in stage-discharge relationships under UGVF conditions. Additional diagnostic relationships of this type should be systematically tested across a wider range of hydrologic and geomorphic settings to better quantify hysteresis occurrence and severity. Such efforts would provide valuable guidance regarding the need for implementing alternative monitoring approaches, such as HyGage, at both existing and future stream-gaging stations.

Table 4. Features of the HyGage measured data that broaden their significance and usage

#	HyGage data features	HyGage data significance & usage
1	Use of Eq. (1) as base for HyGage method accounts for gradual variation of the flow stage in space and time	The method captures accurately discharges during unsteady and gradually varied flows (UGVF)as well as in various combinations of these flow regimes
2	Use of an analytical relationship between measured variables and their gradients	Elimination of empirical adjustment factors and of statistical tools that are not always physically justifiable. The streamflow monitoring equations are akin to those used in numerical modeling of ST-GVFs.
3	Precise estimation of the peak discharge magnitude and timing (missed by HQRC)	Improvement of data accuracy for calibration/validation of rainfall-runoff and flood routing models and for their assimilation in streamflow forecasting models
4	Precise indication of the magnitude and arrival time for the flood crest	Re-evaluation of the methodology for estimation of peak flow, flow volumes and loads of transported matter (particulate and in suspension) during ST-GVFs
5	Continuous data over the whole duration of ST-GVFs	Reducing the errors introduced by extrapolation of the HQRC ratings at higher flow regimes
6	Capturing the phasing of the peak variable hydrographs	The inherent hydrograph succession (i.e., FSS, velocity, stage) in ST-GVFs can be used to flag the subsequent occurrence of the flood crest timing
7	Inclusion of the directly measured derivative $\partial h/\partial x$	The measured derivative $\partial h/\partial x$ enables calculation of $\partial^2 h/\partial x^2$ during a ST-GVF event. The inflexion points in the representation of $\partial^2 h/\partial x^2$ are related to critical control points in the progression of the primitive variable hydrographs.
8	Inclusion of directly measured $\partial V/\partial x$ and $\partial \mathrm{V}/\partial \mathrm{t}$ gradients	The rate changes are direct reflection of reach- or local spatial changes occurring at the station. Their presence can warn that additional site inspections are needed to verify the validity of the initial gaging site conditions.

CONCLUSION

The HyGage monitoring method described in this study belongs to the family of dynamic discharge estimation approaches examined through numerical simulations by Dottori et al. (2009) and applied in situ through the semi empirical protocols of the index velocity method (Levesque & Oberg, 2012) and the continuous slope area method (Smith et al., 2010). These approaches have gained prominence among monitoring agencies, particularly at sites where hysteresis poses challenges to conventional stage–discharge techniques. HyGage advances this approach by integrating components of both methods within a unified, physically based framework and by eliminating the dependence on semi empirical rating curves. A further improvement for HyGage implementation is the incorporation of the entropy-based conversion of the index velocity to mean cross sectional velocity with minimum data input.

The comparative analysis presented in this paper—featuring the index velocity method, the continuous slope area method, and the rating independent HyGage formulation—demonstrates the ability of these approaches to capture hysteretic behavior characteristic of spatiotemporal gradually varied flow. These features, routinely overlooked by the widely used stage–discharge rating curve method, are resolved by HyGage without sacrificing applicability under steady flow conditions. Indeed, when the gradients in Eq. (1) become negligible, the HyGage discharge formulation converges to the conventional stage–discharge relationship, which has been extensively validated for such regimes.

Although the primary objective of this paper is to evaluate the capacity of HyGage to accurately characterize gradually varied flows, the departures between HyGage derived discharges and those obtained from traditional stage–discharge relations remain modest at the analyzed sites due to their mildly hysteretic nature. Nonetheless, the presence of distinct hysteretic patterns across both rising and falling hydrograph limbs underscores the value of HyGage for capturing the full dynamics of fluvial wave propagation. The HyGage capability to distinguish subtle flow mechanisms in ST-GVFs is essential for improving the efficiency, reliability, and operational utility of hydrometric data, thereby enabling enhanced situational awareness, more accurate streamflow forecasting, and more informed decision making across a broad range of riverine environments.

Recent advances in sensing technologies—many capable of measuring stage, index velocity, and free surface slope within a single instrument and deployable across submerged, close range, and remote sensing platforms—position HyGage as a highly adaptable framework for quantifying the primitive variables necessary for discharge estimation in real time. Given the HyGage operational flexibility and the hydrometric community's growing shift toward dynamic, physics-based methods, future studies are expected to build on the analytical framework presented here to ensure robust operational deployment of HyGage that aligns with contemporary scientific standards and continuing to expand its capabilities to new fit-for-purpose applications.

Acknowledgements

This work was supported by the National Science Foundation (NSF-EAR-HS 2139649) and by the National Oceanic and Atmospheric Administration (NOAA) through the Cooperative Institute for Research on Hydrology (CIROH), under the NOAA Cooperative Agreement with The University of Alabama (NA22NWS4320003). We are grateful for the steady and invaluable support for setting instrumentation at the Oxford site provided by our colleagues: Loeser T., Everhart R., Lamoreaux, A., Barquist B. (IIHR-Hydroscience & Engineering), and Lynch M. (Xylem/Sontek).

References

Andreadis, K.M., Coss, S.P., Durand, M., Gleason, C.J., Simmons, T.T., Tebaldi, N., et al., 2025. A first look at river discharge estimation from SWOT satellite observations. *Geophysical Research Letters* 52, e2024GL114185. https://doi.org/10.1029/2024GL114185

Aricò, C., Nasello, C., Tucciarelli, T., 2009. Using unsteady-state water level data to estimate channel roughness and discharge hydrograph. *Advances in Water Resources* 32(8), 1223–1240. https://doi.org/10.1016/j.advwatres.2009.05.001

Bahmanpouri, F., Barbetta, S., Gualtieri, C., Ianniruberto, M., Filizola, N., Termini, D., Moramarco, T., 2022. Prediction of river discharges at confluences based on Entropy theory and surface-velocity measurements. *Journal of Hydrology* 606, 127404. https://doi.org/10.1016/j.jhydrol.2021.127404

Bauer-Gottwein, P., Christoffersen, L., Musaeus, A., Frías, M.C., Nielsen, K., 2024. Hydraulics of time-variable water surface slope in rivers observed by satellite altimetry. *Remote Sensing* 16(21), 4010. https://doi.org/10.3390/rs16214010

Beven, K., 2006. Searching for the Holy Grail of scientific hydrology: Qt = (S, R, Δt)A as closure. *Hydrology and Earth System Sciences* 10, 609–618. https://doi.org/10.5194/hess-10-609-2006

Beven, K., 2016. Facets of uncertainty: epistemic uncertainty, non-stationarity, likelihood, hypothesis testing, and communication. *Hydrological Sciences Journal* 61(9), 1652–1665. https://doi.org/10.1080/02626667.2015.1031761

Chiu, C.-L., 1988. Entropy and 2-D velocity distribution in open channels. *Journal of Hydraulic Engineering* 114(7), 738–756. https://doi.org/10.1061/(ASCE)0733-9429(1988)114:7(738)

Chiu, C.-L., 1989. Velocity distribution in open channels. *Journal of Hydraulic Engineering* 115(5), 576–594. https://doi.org/10.1061/(ASCE)0733-9429(1989)115:5(576)

Dalrymple, T., Benson, M.A., 1967. Measurement of peak discharge by the slope-area method. *U.S. Geological Survey Techniques of Water-Resources Investigations*, book 3, chap. A2, 12 pp. https://doi.org/10.3133/twri03A2

Darienzo, M., Renard, B., Le Coz, J., Lang, M., 2021. Detection of stage-discharge rating shifts using gaugings: A recursive segmentation procedure accounting for observational and model uncertainties. *Water Resources Research* 57, e2020WR028607. https://doi.org/10.1029/2020WR028607

Dhote, P.R., Agarwal, A., Paris, A., Singhal, G., Thakur, P.K., Oubanas, H., et al., 2025. Unveiling the first impressions of the wide-swath altimetry SWOT mission over the Ganga River, India. *Geophysical Research Letters* 52, e2025GL115402. https://doi.org/10.1029/2025GL115402

Di Baldassarre, G., Montanari, A., 2009. Uncertainty in river discharge observations: A quantitative analysis. *Hydrology and Earth System Sciences* 13(6), 913–921. https://doi.org/10.5194/hess-13-913-2009

Domanski, M.M., Holmes, R.R., Jr., Heal, E.N., Knight, T.M., 2025. Dynamic rating method for computing discharge and stage from time-series data. *U.S. Geological Survey Scientific Investigations Report* 2024–5129, 92 pp. https://doi.org/10.3133/sir20245129

Dottori, F., Martina, L.V., Todini, E., 2009. A dynamic rating curve approach to indirect discharge measurements. *Hydrology and Earth System Sciences* 13, 847–863. https://doi.org/10.5194/hess-13-847-2009

Dottori, F., Szewczyk, W., Ciscar, J.-C., Zhao, F., Alfieri, L., Hirabayashi, Y., et al., 2018. Increased human and economic losses from river flooding with anthropogenic warming. *Nature Climate Change* 8(9), 781–786. https://doi.org/10.1038/s41558-018-0257-z

Dykstra, S.L., Dzwonkowski, B., 2020. The propagation of fluvial flood waves through a backwater-estuarine environment. *Water Resources Research* 56, e2019WR025743. https://doi.org/10.1029/2019WR025743

Faye, R.E., Cherry, R.N., 1980. Channel and dynamic flow characteristics of the Chattahoochee River, Buford Dam to Georgia Highway 141. *U.S. Geological Survey Water-Supply Paper* 2063. https://doi.org/10.3133/wsp2063

Fenton, J.D., 2018. On the generation of stream rating curves. *Journal of Hydrology* 564, 748–757. https://doi.org/10.1016/j.jhydrol.2018.07.025

Fenton, J.D., 2025. Velocity distributions in open channels and the calculation of discharge. *Journal of Irrigation and Drainage Engineering* 151(2). https://doi.org/10.1061/JIDEDH.IRENG-10426

Ferrick, M.G., 1985. Analysis of river wave types. *Water Resources Research* 21(2), 209–220. https://doi.org/10.1029/WR021i002p00209

Fread, D.L., 1975. Computation of stage-discharge relationship affected by unsteady flow. *Water Resources Bulletin* 11(2), 213–228. https://doi.org/10.1111/j.1752-1688.1975.tb00674.x

Henderson, F.M., 1966. *Open channel flow*. Macmillan Company, New York, NY, 522 pp.

Herschy, R.W., 2009. *Streamflow measurement* (3rd ed.). CRC Press. https://doi.org/10.1201/9781482265880

Hoitink, A.J.F., 2018. Monitoring and analysis of lowland river discharge. In: *Proceedings of the River Flow Conference* (IAHR), 5–8 September 2018, Lyon, France. *E3S Web of Conferences* 40, 06045. https://doi.org/10.1051/e3sconf/20184006045

Holmes, R.R., 2016. River rating complexity. In: *Proceedings of the River Flow Conference*. Taylor & Francis Group, St. Louis, MO, USA. ISBN 978-1-138-02913-2.

House, E., Kim, K., Muste, M., Meselhe, E., Demir, I., 2025a. Back to basics: On the proper determination of free-surface slope (FSS) in gradually varied open channel flows. *Flow Measurement and Instrumentation* 106, 102979. https://doi.org/10.1016/j.flowmeasinst.2025.102979

House, E., Meselhe, E., Muste, M., Demir, I., 2025b. Streamflow hysteresis analysis through a deep-dive budget of the St Venant equation momentum terms. *Water Resources Research* 61, e2024WR038103. https://doi.org/10.1029/2024WR038103

Ikhouane, F., 2013. Characterization of hysteresis process. *Mathematics of Control, Signals, and Systems* 25, 291–310. https://doi.org/10.1007/s00498-012-0099-6

ISO, 1992. Liquid flow measurement in open channels – Slope-area method. ISO 1070:1992, International Organization for Standardization, Geneva. https://www.iso.org/standard/5564.html

Johnson, E.D., Cowen, E.A., 2017. Remote determination of the velocity index and mean streamwise velocity profiles. *Water Resources Research* 53, 7521–7535. https://doi.org/10.1002/2017WR020504

Kechnit, D., Tshimanga, R.M., Ammari, A., Trigg, M.A., Carr, A.B., Bahmanpouri, F., Barbetta, S., Moramarco, T., 2024. Bathymetry and discharge estimation in large and data-scarce rivers using an entropy-based approach. *Hydrological Sciences Journal* 69(15), 2109–2123. https://doi.org/10.1080/02626667.2024.2402933

Kennedy, E.J., 1984. Discharge ratings at gaging stations. *U.S. Geological Survey Techniques of Water-Resources Investigations*, book 3, chap. A10, 59 pp. https://doi.org/10.3133/twri03A10

Kim, K., Muste, M., Hauet, A., 2025. Analytical estimation of cross-sectional velocity distribution using index-velocity acquired with horizontal Acoustic Doppler Current Profilers (H-ADCP). *AGU Fall Meeting*, 15–19 December 2025, New Orleans, LA.

Kreibich, H., Van Loon, A.F., Schröter, K., Ward, P.J., Mazzoleni, M., Sairam, N., et al., 2022. The challenge of unprecedented floods and droughts in risk management. *Nature* 608(7921), 80–86. https://doi.org/10.1038/s41586-022-04917-5

Laenen, A., 1985. Acoustic velocity meter systems. *U.S. Geological Survey Techniques of Water-Resources Investigations*, book 3, chap. A17, 38 pp. https://doi.org/10.3133/twri03A17

Le Coz, J., Pierrefeu, G., Paquier, A., 2008. Evaluation of river discharges monitored by a fixed side-looking Doppler profiler. *Water Resources Research* 44, W00D09. https://doi.org/10.1029/2008WR006967

Lee, K., Firoozfar, A.R., Muste, M., 2017. Monitoring of unsteady open channel flows using continuous slope-area method. *Hydrology and Earth System Sciences* 21, 1863–1874. https://doi.org/10.5194/hess-21-1863-2017

Lee, K., Muste, M., 2017. Refinement of the Fread method for improved tracking of stream discharges during unsteady flows. *Journal of Hydraulic Engineering* 143(6). https://doi.org/10.1061/(ASCE)HY.1943-7900.0001280

Levesque, V.A., Oberg, K.A., 2012. Computing discharge using the index velocity method. *U.S. Geological Survey Techniques and Methods*, book 3, chap. A23. https://doi.org/10.3133/tm3A23

Litrico, X., Fromion, V., 2009. *Modeling and control of hydrosystems*. Springer, 409 pp. https://doi.org/10.1007/978-1-84882-624-3

McMillan, H., Seibert, J., Petersen-Øverleir, A., Lang, M., White, P., Snelder, T., et al., 2017. How uncertainty analysis of streamflow data can reduce costs and promote robust decisions in water management applications. *Water Resources Research* 53, 5220–5228. https://doi.org/10.1002/2016WR020328

Moramarco, T., Saltalippi, C., Singh, V.P., 2004. Estimation of mean velocity in natural channel based on Chiu's velocity distribution equation. *Journal of Hydrologic Engineering* 9(1), 42–50. https://doi.org/10.1061/(ASCE)1084-0699(2004)9:1(42)

Moramarco, T., Pandolfo, C., Singh, V.P., 2008. Accuracy of kinematic wave and diffusion wave approximations for flood routing. I: Steady analysis. *Journal of Hydrologic Engineering* 13(11), 1078–1088. https://doi.org/10.1061/(ASCE)1084-0699(2008)13:11(1078)

Moramarco, T., Barbetta, S., Tarpanelli, A., 2017. From surface velocity measurements to discharge assessment by entropy theory. *Water* 9(2), 120. https://doi.org/10.3390/w9020120

Moramarco, T., Barbetta, S., Bjerklie, D.M., Fulton, J., Tarpanelli, A., 2019. River bathymetry estimate and discharge assessment from remote sensing. *Water Resources Research* 55, 6692–6711. https://doi.org/10.1029/2018WR024220

Moussa, R., Bocquillon, C., 1996. Criteria for the choice of flood-routing methods in natural channels. *Journal of Hydrology* 186(1–4), 1–30. https://doi.org/10.1016/S0022-1694(96)03045-4

Muste, M., Bacotiu, C., Thomas, D., 2019. Evaluation of the slope-area method for continuous streamflow monitoring. In: *Proceedings of the 38th IAHR World Congress*, 1–6 September 2019, Panama City, Panama.

Muste, M., Lee, K., Kim, D., Bacotiu, C., Rojas Oliveros, M., Cheng, Z., Quintero, F., 2020. Revisiting hysteresis of flow variables in monitoring unsteady streamflows. *Journal of Hydraulic Research* 58(6), 867–887. https://doi.org/10.1080/00221686.2020.1786742

Muste, M., Kim, D., Kim, K., 2022a. A flood-crest forecast prototype for river floods using only in-stream measurements. *Communications Earth & Environment* 3(1), 78. https://doi.org/10.1038/s43247-022-00402-z

Muste, M., Kim, D., Kim, K., 2022b. Insights into flood wave propagation in natural streams as captured with acoustic profilers at an index-velocity gaging station. *Water* 14(9), 1380. https://doi.org/10.3390/w14091380

Muste, M., 2023. Novel physically-based streamflow monitoring methodology. CIROH Award NA22NWS4320003, National Weather Service/National Oceanic and Atmospheric Administration.

Muste, M., Kim, K., Kim, D., Fleit, G., 2025a. Decoding the hysteretic behavior of hydraulic variables in lowland rivers with multivariate monitoring approaches. *Hydrological Processes*. https://doi.org/10.1002/hyp.70008

Muste, M., Kim, K., Kim, D., Demir, I., 2025b. Comparative analysis of the stage-discharge rating operated in gradual varied flows with alternative streamflow monitoring approaches. Preprint, *EarthArXiv*. https://doi.org/10.31223/X52Q7X

Nihei, Y., Kimizu, A., 2008. A new monitoring system for river discharge with horizontal acoustic Doppler current profiler measurements and river flow simulation. *Water Resources Research* 44, W00D20. https://doi.org/10.1029/2008WR006970

Perret, E., Lang, M., Le Coz, J., 2022. A framework for detecting stage-discharge hysteresis due to flow unsteadiness: Application to France's national hydrometry network. *Journal of Hydrology* 608, 127567. https://doi.org/10.1016/j.jhydrol.2022.127567

Perumal, M., Shrestha, K.B., Chaube, U.C., 2004. Reproduction of hysteresis in rating curves. *Journal of Hydraulic Engineering* 130(9), 870–878. https://doi.org/10.1061/(ASCE)0733-9429(2004)130:9(870)

Petersen-Øverleir, A., 2006. Modelling stage–discharge relationships affected by hysteresis using the Jones formula and nonlinear regression. *Hydrological Sciences Journal* 51(3), 365–388. https://doi.org/10.1623/hysj.51.3.365

Prowse, C.W., 1984. Some thoughts on lag and hysteresis. *Area* 16(1), 17–23.

Rantz, S.E., et al., 1982. Measurement and computation of streamflow. *U.S. Geological Survey Water-Supply Paper* 2175, Vols. 1–2. https://doi.org/10.3133/wsp2175

Rátky, I., 2000. Árvízi hurokgörbék közelítő számítása. *Vízügyi Közlemények* 82(2), 232–261 (in Hungarian).

Rozos, E., Leandro, J., Koutsoyiannis, D., 2022. Development of rating curves: Machine learning vs. statistical methods. *Hydrology* 9(10), 166. https://doi.org/10.3390/hydrology9100166

Saint-Venant, A.J.C. Barré de, 1871. Théorie du mouvement non permanent des eaux, avec application aux crues des rivières et à l'introduction de marées dans leurs lits. *Comptes Rendus de l'Académie des Sciences* 73, 147–154 and 237–240.

Schmidt, A.R., 2002. Analysis of stage-discharge relations for open-channel flows and their associated uncertainties. Ph.D. thesis, University of Illinois at Urbana–Champaign, Urbana, IL.

Schmidt, A.R., Garcia, M.H., 2003. Theoretical examination of historical shifts and adjustments to stage-discharge rating curves. In: *ASCE World Water & Environmental Resources Congress*, Philadelphia, PA.

Schwatke, C., Halicki, M., Scherer, D., 2024. Generation of high-resolution water surface slopes from multi-mission satellite altimetry. *Water Resources Research* 60, e2023WR034907. https://doi.org/10.1029/2023WR034907

Sichangi, A.W., Wang, L., Hu, Z., 2018. Estimation of river discharge solely from remote-sensing derived data: An initial study over the Yangtze River. *Remote Sensing* 10(9), 1385. https://doi.org/10.3390/rs10091385

Singh, V.P., 2025. Entropy in hydrology. *Perspectives of Earth and Space Scientists* 6, e2025CN000272. https://doi.org/10.1029/2025CN000272

Smith, C.F., Cordova, J.T., Wiele, S.M., 2010. The continuous slope-area method for computing event hydrographs. *U.S. Geological Survey Scientific Investigations Report* 2010–5241, 37 pp. https://doi.org/10.3133/sir20105241

Spada, E., Sinagra, M., Tucciarelli, T., Biondi, D., 2017. Unsteady state water level analysis for discharge hydrograph estimation in rivers with torrential regime: The case study of the February 2016 flood event in the Crati River, South Italy. *Water* 9(4), 288. https://doi.org/10.3390/w9040288

Tayfur, G., Moramarco, T., 2022. Kinematic reverse flood routing in natural rivers using stage data. *Applied Water Science* 12, 182. https://doi.org/10.1007/s13201-022-01707-2

Tsubaki, R., Moramarco, T., Manatis, G., Le Coz, J., Muste, M., 2025. Advances in river measurement technologies. Invited paper, *New Waves in Hydrometry (Japan)* 1, 36–59.

USGS, 2010. Continuous records processing of all water time series data. Water Resources Discipline Policy Memorandum 2010.02, U.S. Geological Survey. http://water.usgs.gov/admin/memo/policy/wrdpolicy10.02.html

USPTO, 2026. Measurement system for streamflow determination in real time. U.S. Patent No. 12,529,586, University of Iowa Research Foundation, United States Patent and Trademark Office, January 20, 2026.

Wang, Y., Morton, Y.J., Minear, J.T., Putnam, A., Conrad, A., Axelrad, P., Nerem, R.S., Warnock, A., Ruf, C., Moreira, D.M., Talpe, M., 2025. Measuring river slope using spaceborne GNSS reflectometry: Methodology and first performance assessment. *Remote Sensing of Environment* 318, 114597. https://doi.org/10.1016/j.rse.2025.114597

Westerberg, I.K., Karlsen, R.H., 2024. Sharing perceptual models of uncertainty: On the use of soft information about discharge data. *Hydrological Processes* 38(5), e15145. https://doi.org/10.1002/hyp.15145

WSDOT, 2025. *Hydraulics manual*, M23-03.11. Washington State Department of Transportation, Olympia, WA.

Yu, C.-W., Hodges, B.R., Liu, F., 2020. A new form of the Saint-Venant equations for variable topography. *Hydrology and Earth System Sciences* 24, 4001–4024. https://doi.org/10.5194/hess-24-4001-2020